Princeton Plasma Physics Laboratory

PPPL- 4811

PPPL- 4811

Application of Spatially Resolved High Resolution Crystal Spectrometry to ICF Plasmas

Kenneth W. Hill, M. Bitter, L. Delgado-Aprico, N.A. Pablant, P. Beiersdorfer, M. Schneider, K. Widmann, M. Sanchez del Rio and L. Zhang

September, 2012

PPPL PRINCETON PLASMA PHYSICS LABORATORY

Prepared for the U.S. Department of Energy under Contract DE-AC02-09CH11466.

Princeton Plasma Physics Laboratory
Report Disclaimers

Full Legal Disclaimer

Trademark Disclaimer

PPPL Report Availability

Princeton Plasma Physics Laboratory:

http://www.pppl.gov/techreports.cfm

Office of Scientific and Technical Information (OSTI):

http://www.osti.gov/bridge

Related Links:

U.S. Department of Energy

Office of Scientific and Technical Information

Fusion Links

Application of spatially resolved high resolution crystal spectrometry to inertial confinement fusion plasmas[a)]

K. W. Hill,[1,b)] M. Bitter,[1] L. Delgado-Aparacio,[1] N. A. Pablant,[1] P. Beiersdorfer,[2] M. Schneider,[2] K. Widmann,[2] M. Sanchez del Rio,[3] and L. Zhang[4]
[1]*Princeton Plasma Physics Laboratory, Princeton, New Jersey 08543, USA*
[2]*Physics Division, Lawrence Livermore National Laboratory, Livermore, California 94550, USA*
[3]*European Synchrotron Radiation Facility, BP 220, 38043-Grenoble Cedex, France*
[4]*Institute of Plasma Physics, Chinese Academy of Sciences, Hefei 230031, China*

(Presented 7 May 2012; received 4 May 2012; accepted 25 June 2012; published online 3 August 2012)

High resolution ($\lambda/\Delta\lambda \sim 10\,000$) 1D imaging x-ray spectroscopy using a spherically bent crystal and a 2D hybrid pixel array detector is used world wide for Doppler measurements of ion-temperature and plasma flow-velocity profiles in magnetic confinement fusion plasmas. Meter sized plasmas are diagnosed with cm spatial resolution and 10 ms time resolution. This concept can also be used as a diagnostic of small sources, such as inertial confinement fusion plasmas and targets on x-ray light source beam lines, with spatial resolution of micrometers, as demonstrated by laboratory experiments using a 250-μm ^{55}Fe source, and by ray-tracing calculations. Throughput calculations agree with measurements, and predict detector counts in the range 10^{-8}–10^{-6} times source x-rays, depending on crystal reflectivity and spectrometer geometry. Results of the lab demonstrations, application of the technique to the National Ignition Facility (NIF), and predictions of performance on NIF will be presented. © *2012 American Institute of Physics*. [http://dx.doi.org/10.1063/1.4738651]

I. INTRODUCTION

High resolution one-dimensionally (1D) x-ray imaging spectrometers (XICS) are used routinely to measure spatial profiles of ion temperature (T_i), plasma flow velocity (v), and electron temperature (T_e), specifically toroidal plasma rotation, in tokamaks in four countries,[1–5] and this instrument is a primary diagnostic for measurement of profiles of T_i and v for the international tokamak, ITER.[6,7] High spectral resolving power ($\lambda/\Delta\lambda \sim 10\,000$) enables precise measurement of these parameters via Doppler broadening, Doppler wavelength shifts, and ratios of dielectronic satellite intensity to resonance line intensity, respectively, usually of 1*s*–2*p* x-ray lines in He-like and H-like ions, such as Ar. The XICS has enabled a revitalization of and significant advances in such important physics phenomena as intrinsic or self-generated flows,[8] flows generated by RF current drive,[9–11] thermal and particle transport,[12] and impurity transport.[13] The continuous spatial resolution enables detailed comparisons of measured phenomena with theoretical predictions, such as turbulent fluctuation induced thermal and impurity transport. In tokamaks, the entire minor cross section, which is of order 1 m high, can be imaged with spatial resolution of order 1 cm, limited by the large size of the plasma and the crystal height.

The XICS concept can also be applied with significant advantages to diagnose small x-ray sources, such as high energy density plasmas (HEDP), and synchrotron x-ray experiments, such as x-ray fluorescence micro-tomography, with equally high spectral resolution. Other groups have previously demonstrated spatially resolved spectroscopy of HED plasmas using spherically bent crystals, e.g., Ref. 14 but have not, to our knowledge, used the precise geometry that we employ. We use large radii (>60 cm) precision spherically bent perfect crystals at Bragg angles 53°–60° with the source at the sagittal focus and detector on the Rowland circle. With this geometry, good spectral resolution is realized regardless of source size or location.

This work investigates the limiting spatial resolution of a high spectral resolution XICS for small sources, and accurate prediction of the throughput to enable designing a useful instrument for HEDP diagnosis. Much previously reported high resolution spectroscopy of emission and absorption lines in HED plasmas has been limited to resolving powers of order 1000 or less,[15,16] and the improved resolving power of our XICS concept is likely to enable more precise measurement of x-ray line shapes and, hopefully, result in a better understanding of the physical processes such as Doppler and Stark broadening which affect the line shape. A major advantage for NIF is that the crystal and detector of the XICS could be located well outside the target chamber to enable extensive shielding of the detector from high yield neutrons, as well as hard x rays.

II. EXPERIMENT

A. Apparatus

The spatially resolving spectrometer consists of a spherically bent x-ray diffracting crystal and a two-dimensional (2D) photon-counting detector. The spherical crystal provides

[a)]Contributed paper, published as part of the Proceedings of the 19th Topical Conference on High-Temperature Plasma Diagnostics, Monterey, California, May 2012.
[b)]Author to whom correspondence should be addressed. Electronic mail: khill@pppl.gov.

spectral dispersion and focusing of the x rays from the source onto the detector in the dispersion plane, a horizontal plane in our case, and images the x rays in the orthogonal (vertical) plane. To obtain good spatial resolution for small scale plasmas the x-ray source is placed on the sagittal focal line of the spherical crystal at a distance

$$f_s = -\frac{R\sin\theta}{\cos 2\theta} \quad (1)$$

from the crystal, where R is the radius of curvature of the crystal, and θ is the Bragg angle, or angle between the x-ray path and the plane of the crystal at its center. The 2D detector is placed on the Rowland circle at a distance

$$f_m = R\sin\theta \quad (2)$$

from the crystal. For our experiments a quartz crystal, spherically bent to a radius of 75.8 cm, and having a height of 8 cm and a width of 4 cm was used.

For the initial experiments reported here, Mn Kα lines from an ^{55}Fe radioactive source were analyzed in second order from the 110 planes at a Bragg angle of 59°. To simulate a small scale HED plasma the 5-mm diameter source was covered by a plate having a slit of width 250 μm, with the length of the slit oriented horizontally. The source, located at the sagittal focal distance of ~136 cm from the crystal, was placed on a vertical micrometer translation stage and was translated vertically in 10-μm steps, which was the smallest division on the micrometer scale. The low x-ray intensity from the ^{55}Fe source did not permit measurements with smaller slits. In future experiments we will use a 5–7 μm spot size micro-focus x-ray tube to do finer scale spatial imaging experiments.

The detector, a Pilatus 100 k 2D hybrid pixel array detector, having a pixel size of 172 μm, was located on the Rowland circle at a distance of $f_m \sim 65$ cm from the crystal. The spatial demagnification factor, f_s/f_m, of the imaging spectrometer was about 2.1, so that the 250-mm high apertured source was de-magnified to an image of ~120-μm height which was spectrally dispersed in the horizontal plane. As the source was translated vertically in 10-μm steps, the image was also translated vertically, in the opposite sense, in 5-μm steps.

B. Spectral-spatial image

A contour plot of the spectrally-spatially resolved image of the ^{55}Fe source is shown in Fig. 1 for the case when

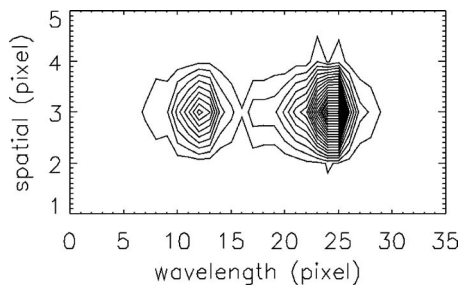

FIG. 1. Spectral-spatial image of Mn Kα_1 (right) and Kα_2 (left) x-ray lines emitted from apertured ^{55}Fe source.

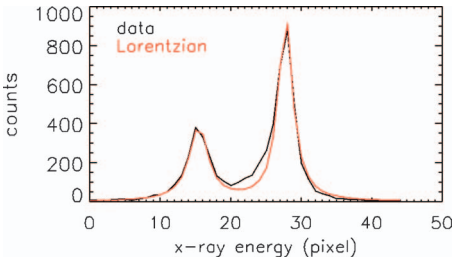

FIG. 2. Mn Kα x-ray spectrum measured using the spatially spectrally resolving x-ray spectrometer. The left peak is Kα_2 and the right peak is Kα_1.

the spectral image was focused primarily on spatial pixel row number 3 of the Pilatus 100 k detector. Eighty-five percent of the intensity is in row 3, and the remaining intensity is equally distributed in rows 2 and 4.

When the spectral image of Fig. 1 is summed vertically the spectrum illustrated in Fig. 2 is obtained. The black curve is the measured data and the red curve is a Lorentzian function. The inferred line widths of the Kα_1 (taller peak) and Kα_2 peaks are 2.28 eV and 2.96 eV, respectively, which agree with available measurements of the natural line widths[17] within 0.02 eV and 0.04 eV, respectively, suggesting that the instrumental contribution to the line width is small. The feature in the vicinity of spectral pixels 20–25 in the measured curve can be attributed to chemical shifts of the Mn energy levels in the Fe-Mn matrix; similar effects have been seen in Mn Kα and Kβ x rays, and the amplitude of the raised feature varies with valence state for Mn in different compounds such as Mn(II)O, Mn(IV)O_2, and KMn(VII)O_4.[18]

C. Spatial resolution

As a preliminary test of the spatial resolution of our 1D imaging spectrometer for small scale sources, we translated the 120-μm wide x-ray image in ~5-μm steps across the boundary between two rows of pixels on the Pilatus detector. The position of the image from the boundary is given by x = L*N1/(N1+N2), where L is the 120-μm width of the image, and N1 and N2 are the total counts recorded in pixel rows 1 and 2, respectively.

The results of this spatial scan are shown in Fig. 3. The average deviation from the straight line is only a few micrometers, and could result partially from errors in setting the micrometer to its smallest division, which is 10 μm, and

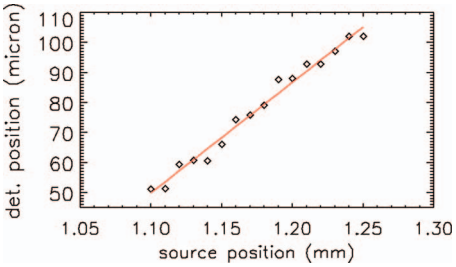

FIG. 3. Inferred position of ~120-mm high x-ray image on Pilatus detector as a function of the 250-mm high x-ray source, as the source is translated vertically in 10-μm steps.

statistical errors of a few percent, resulting from the total counts of ~1100 per experiment. While these measurements do not prove that the spectrometer can provide small scale spatial resolution down to the 1-μm level, they are suggestive of this possibility. Future experiments will be done with a 5-μm micro-focus x-ray tube using detectors with 15-μm pixel size.

D. X-ray throughput of spectrometer

The measured x-ray counts, N′, agree within 20% with the counts predicted by the theoretical expression

$$N' = \frac{N}{4\pi} I_{ref} \frac{H}{R} \frac{\cos(2\theta_0)}{\cos(\theta_0)\tan(2\theta_0)}, \quad (3)$$

where N is the number of counts emitted by the source, H is the height of the crystal, I_{ref} is the integrated reflectivity of the crystal, R is the radius of curvature, and θ_0 is the Bragg angle. For the quartz (110) crystal in second order, the integrated reflectivity is about 15 microradians at 5.9 keV.

For our parameters, the ratio N′/N is predicted to be about 1.03×10^{-7}, and the predicted count rate is about 1.1 counts/s. The 20% deficit in the measured count rate is attributable to aging of the radioactive source and attenuation in windows, the long helium path, and short air paths. Note that if we used a Ge [331] crystal we would have a factor of three times higher throughput at a Bragg angle of 54°.

III. SUMMARY

The spatially imaging x-ray crystal spectrometer, consisting of a spherically bent crystal and a 2D imaging x-ray detector, is simple in design, and can potentially be adapted to sources of different sizes, from micrometers to millimeters to meters. It provides excellent spectral resolution and can also provide spatial resolution down to the scale of micrometers. This type of diagnostic could potentially add new understanding to HED physics and has the potential to significantly speed up experiments on high brightness x-ray sources by allowing simultaneous spatial and spectral measurements. The angular alignment (pointing) of the spectrometer relative to the small source is simple if the detector dimensions are centimeters, because of the imaging properties in one dimension, and because the point image needs only to be located on the few cm long sagittal focal line in the perpendicular dimension. The 20% deficit in the measured count rate is attributable to aging of the radioactive source and attenuation in windows, the long helium path, and short air paths. The throughput ranges from 10^{-8} to 10^{-6} detector photons per source photon for typical crystal reflectivities and geometries.

As a practical example we consider a NIF exploding pusher with 500-μm diameter, Te = 5 keV, electron density = 5.34×10^{22} cm^{-3}, and with a Kr dopant of 0.01% of n_e. The FLYCHK code predicts 4×10^{12} photons/sr in the He-like Kr resonance line "w" at 13.1 keV in one ps, or about 5×10^{13} total photons in one ps. Thus, from Eq. (3), we predict about 6000 photons/ps on the detector from a 10-cm high Ge [844] crystal, which has an integrated reflectivity of about 2.5×10^{-6} radians at 13.1 keV. This 6000 phonons/ps allows us to measure line shapes with a 2% error in one ps, assuming a suitable detector with ps time resolution becomes available.[19]

In future experiments, more definitive spatial-resolution measurements will be made by replacing the 250-μm source by a Hamamatsu x-ray tube with 5-μm x-ray spot size, and replacing the Pilatus detector, having 172 μm pixels, by both a Medipix2 detector with 55-μm pixel size and a Princeton instruments x-ray CCD having 15-μm pixels.

ACKNOWLEDGMENTS

This work was performed under the auspices of the (U.S.) Department of Energy (DOE) by Princeton Plasma Physics Laboratory (PPPL) under Contract No. DE- ACO2-76-CHO-3073 and Lawrence Livermore National Laboratory (LLNL) under Contract No. DE-AC52-07NA-27344.

[1] A. Ince-Cushman, J. E. Rice, M. Bitter, M. L. Reinke, K. W. Hill *et al.*, Rev. Sci. Instrum. **79**, 10E302 (2008).
[2] K. W. Hill, M. L. Bitter, S. D. Scott, A. Ince-Cushman, M. Reinke *et al.*, Rev. Sci. Instrum. **79**, 10E320 (2008).
[3] Y. Shi, F. Wang, B. Wan, M. Bitter, S. G. Lee, J. Bak, K. Hill, J. Fu, Y. Li, A. Ti, and B. Ling, Plasma Phys. Control. Fusion **52**, 085014 (2010).
[4] S. G. Lee, J. G. Bak, U. W. Nam, M. K. Moon, Y. Shi, M. Bitter, and K. W. Hill, Rev. Sci. Instrum. **81**, 10E506 (2010).
[5] N. A. Pablant, M. Bitter, L. Delgado-Aparicio, M. Goto, K. W. Hill, "Layout and results from the initial operation of the high-resolution x-ray imaging crystal spectrometer on the Large Helical Device, " Rev. Sci. Instrum. (to be published).
[6] P. Beiersdorfer, J. Clementson, J. Dunn, M. F. Gu, K. Morris *et al.*, J. Phys. B **43**, 144008 (2010).
[7] K. W. Hill, M. Bitter, L. Delgado-Aparicio, D. Johnson, R. Feder *et al.*, Rev. Sci. Instrum. **81**, 10E322 (2010).
[8] J. E. Rice, J. W. Hughes, P. H. Diamond, Y. Kosuga, Y. A. Podpaly *et al.*, Phys. Rev. Lett. **106**, 215001 (2011).
[9] A. Ince-Cushman, J. E. Rice, M. Reinke, M. Greenwald, G. Wallace *et al.*, Phys. Rev. Lett. **102**, 035002 (2009).
[10] Y. Lin, J. E. Rice, S. J. Wukitch, M. J. Greenwald, A. E. Hubbard, A. Ince-Cushman *et al.*, Phys. Rev. Lett. **101**, 235002 (2008).
[11] Y. Shi, G. Xu, F. Wang, M. Wang, J. Fu, Y. Li, W. Zhang *et al.*, Phys. Rev. Lett. **106**, 235001 (2011).
[12] C. L. Fiore, J. E. Rice, Y. Podpaly, I. O. Bespamyatnov, W. L. Rowan, J. W. Hughes, and M. Reinke, Nucl. Fusion **50**, 064008 (2010).
[13] N. T. Howard, M. Greenwald, D. R. Mikkelsen, A. E. White, M. L. Reinke, D. Ernst, Y. Podpaly, and J. Candy, Phys. Plasmas **19**, 056110 (2012).
[14] P. F. Knapp, S. A. Pikuz, T. A. Shelkovenko, D. A. Hammer, and S. B. Hansen, Rev. Sci. Instrum. **82**, 063501 (2011).
[15] R. Florido, R. C. Mancini, T. Nagayama, R. Tommasini, J. A. Delettrez, S. P. Regan *et al.*, High Energy Density Phys. **6**, 70 (2010).
[16] S. P. Regan, R. Epstein, B. A. Hammel, L. J. Suter, J. Ralph, H. Scott *et al.*, Phys. Plasmas **19**, 056307 (2012).
[17] S. I. Salem and P. L. Lee, At. Data Nucl. Data Tables **18**, 233 (1976).
[18] U. Bergmann, C. R. Horne, T. J. Collins, J. M. Workman, and S. P. Cramer, Chem. Phys. Lett. **302**, 119 (1999).
[19] M. E. Lowry *et al.*, *paper presented at the Ultra Fast Optics Conference, Monterey, California, September 26*, 2011, LLNL-CONF-491441.

The Princeton Plasma Physics Laboratory is operated
by Princeton University under contract
with the U.S. Department of Energy.

Information Services
Princeton Plasma Physics Laboratory
P.O. Box 451
Princeton, NJ 08543

Phone: 609-243-2245
Fax: 609-243-2751
e-mail: pppl_info@pppl.gov
Internet Address: http://www.pppl.gov